electronics

MDPI

Article

Energy-Efficient Power Allocation for Full-Duplex Device-to-Device Underlaying Cellular Networks with NOMA

Xu Zhao [1], Fang Liu [2,*], Yajing Zhang [2], Songchao Chen [2] and Jie Gan [1]

[1] Beijing Smart-Chip Microelectronics Technology Co., Ltd., Beijing 100192, China; zhaoxu@sgchip.sgcc.com.cn (X.Z.); ganjie@sgchip.sgcc.com.cn (J.G.)
[2] School of Electronic Engineering, Beijing University of Posts and Telecommunications, Beijing 100876, China; zyj_bupt@bupt.cn (Y.Z.); csongchao@bupt.edu.cn (S.C.)
* Correspondence: lf@bupt.edu.cn

Abstract: Full-duplex (FD), Device-to-Device (D2D) and non-orthogonal multiple access (NOMA) are promising wireless communication techniques to improve the utilization of spectrum resources. Meanwhile, introducing FD, D2D and NOMA in cellular networks is very challenging due to the complex interference problem. To deal with the complex interference of FD D2D underlaying NOMA cellular networks, power allocation (PA) is extensively studied as an efficient interference management technique. However, most of the previous research works on PA to optimize energy efficiency only consider the system framework of partially joint combining techniques of FD, D2D and NOMA, and the constraints of optimization problem are very different. In this paper, in order to further improve the energy efficiency of a system, a dual-layer iteration power allocation algorithm is proposed to eliminate the complex interference. The outer-layer iteration is to solve the non-linear fractional objective function based on Dinkelbach, and the inner-layer iteration is to solve the non-convex optimization problem based on D.C. programming. Then, the non-convex and non-linear fractional objective function is transformed into a convex function to solve the optimal power allocation. In this approach, FD D2D users reuse the spectrum with downlink NOMA cellular users. Imperfect self-interference (SI) cancellation at the FD D2D users and the successive interference cancellation (SIC) at the strong NOMA user are considered in the system framework. The optimization problem is constructed to maximize the system's energy efficiency with the constraints of successful SIC, QoS requirements, the maximum transmit power of BS and FD D2D users. Numerical results demonstrate that the proposed algorithm outperforms the traditional orthogonal multiple access (OMA) in terms of energy efficiency with a higher system sum rate.

Keywords: non-orthogonal multiple access; full-duplex; Device-to-Device communication; power allocation; energy efficiency

check for updates

Citation: Zhao,X.; Liu, F.; Zhang, Y.; Chen, S.; Gan, J. Energy-Efficient Power Allocation for Full-Duplex Device-to-Device Underlaying Cellular Networks with NOMA. *Electronics* **2023**, *12*, 3433. https://doi.org/10.3390/electronics12163433

Academic Editor: Dimitra I. Kaklamani

Received: 7 July 2023
Revised: 10 August 2023
Accepted: 11 August 2023
Published: 14 August 2023

Copyright: © 2023 by the authors. Licensee MDPI, Basel, Switzerland. This article is an open access article distributed under the terms and conditions of the Creative Commons Attribution (CC BY) license (https://creativecommons.org/licenses/by/4.0/).

1. Introduction

Recently, researchers have growing interest in Device-to-Device (D2D) communications underlaying cellular networks because D2D users can reuse the spectrum of cellular users, thus improving the spectral efficiency [1–4]. Similarly, non-orthogonal multiple access (NOMA) and full-duplex (FD) as significant candidate technologies in 5G can greatly improve the spectrum utilization and achieve a higher energy efficiency for next-generation wireless communication [5–7]. However, the combination of the above three will cause serious co-channel interference while improving spectral efficiency. Therefore, a reasonable resource allocation has become particularly important, which can effectively suppress interference while ensuring the system spectral efficiency. On the other hand, for massive machine-type communications (mMTC) scenario in 5G, users' energy is always limited [8,9]. How to improve energy efficiency while guaranteeing the quality of service (QoS) of equipments is also a key problem.

D2D communication allows users to transmit directly while using the authorized frequency band of the base station (BS), thus reducing the burden of the BS and save communication resources of cellular BS. Therefore, D2D communications can improve the overall capacity of the mobile communication system. For this reason, D2D communication is considered in cellular networks while causing co-channel interference when D2D users multiplex the resources of cellular networks. Resource allocation for D2D communications underlaying cellular networks was researched in [10–15]. In [10], the spectral efficiency of D2D users was maximized. Four transmit power control strategies were proposed, ensuring that the interference to the BS should be lower than a threshold. In [11], the system throughput was maximized while ensuring that the co-channel interference remained minimized. The channel allocation, mode selection and power control were also studied.

NOMA is a promising solution for reducing the co-channel interference using the successive interference cancellation (SIC) at the receivers in 5G. Nowadays, many researches have studied the resource allocation of D2D joint NOMA communications scenarios [16–20]. The maximization of the uplink energy efficiency and the achieved rate of the D2D communication based on the NOMA system were studied in [16]. The authors proposed a joint power control and sub-channel assignment algorithm to gain the optimal energy efficiency. In [17], the authors investigated the time scheduling and resource allocation algorithms in a NOMA-based D2D communication while maintaining energy efficiency among D2D users without affecting cellular users' energy efficiency. In [18], the authors optimized the power allocation, the resource assignment and the SIC decoding order for the NOMA users to maximize the obtained rate of D2D communication.

FD communication allows users to transmit and receive signals using the same spectrum simultaneously, and thus theoretically, the capacity can be twice that of half-duplex (HD) communication with the development of self interference (SI) cancellation technology. The combination of FD and D2D communication joint NOMA has aroused researchers' great interest [21–26]. The NOMA vehicle-to-everything (V2X) system was considered in [21], in which the vehicle enabled the D2D transmission mode. As for the Roadside Unit (RSU) selection, a full-duplex communication mode was applied to further improve the performance. The ergodic rate of two vehicles in a specific group was compared. In [22], the cell-center D2D user acted as the relay for the cell-edge D2D user, while the cell-center D2D user can operate in HD or FD communication mode to communicate and form a group of NOMA users with multiple relay nodes. Three schemes supporting D2D-NOMA systems were proposed to derive the outage probabilities. Cooperative NOMA (C-NOMA) in cellular downlink systems was discussed in [23], in which users operated in FD mode and can assist the communication from the BS to poor-channel-quality users. D2D user grouping and power control were studied to improve multiplexing gain. In addition, some researchers focus on the machine learning [27–30] technique to deal with big data and resolve non-linear problems. In [28], a nature deep Q-Learning algorithm in deep reinforcement learning is proposed to solve the power allocation problem for achieving a higher data rate and energy efficiency of MIMO-NOMA wireless network. In [29], the authors aimed to maximize the total energy efficiency of D2D multicast clusters underlaying cellular networks. Since the optimization problem is non-convex, the authors transform it into a mixed-integer programming problem according to the Dinkelbach algorithm and employing the Q-Learning to solve it. In [30], the authors design a novel artificial intelligence (AI)-based framework for maximizing the secrecy energy efficiency (SEE) in FD cooperative relay underlaying cognitive radio NOMA systems. The non-convex SEE optimization problem is solved with ensemble learning to select the optimal relay and with a quantum particle swarm optimization-based technique to optimize power allocation.

Although the above work has carried out a detailed analysis on the research of D2D, FD and NOMA, there is still little work on the comprehensive combination of D2D, FD and NOMA, which is of great value to promote the system's spectral efficiency and energy efficiency. Motivated by this, we research on the resource allocation of FD D2D underlaying cellular networks with downlink NOMA, where FD D2D users can operate at the

same spectrum with downlink NOMA users. Considering the energy-limited nature of wireless terminal devices and the requirements of global green communication, we set the maximization of the system's energy efficiency as the ultimate goal. At the same time, we consider that the transmission rate is very important to users, because many services such as watching videos, playing online games and live broadcasting do need relatively high data rates. Therefore, we maximize the system's energy efficiency while ensuring users' QoS requirements.

The contributions of this paper can be summarized as follows:

(1) We investigate FD D2D underlaying cellular networks with downlink NOMA, where two downlink cellular users form a group of NOMA users and the FD D2D users reuse the spectrum for NOMA users.
(2) The system's energy efficiency is maximized under the conditions of power constraints for all users, the successful SIC for NOMA users and the QoS requirements for FD D2D users and NOMA users.
(3) The optimization problem in this paper is non-convex and non-linear fractional, which makes it difficult to obtain the optimal solution directly. Thus, a dual-layer iteration algorithm is proposed to deal with the problem. The outer-layer iteration algorithm is to solve a non-linear fractional problem based on Dinkelbach algorithm, and the inner-layer iteration algorithm, based on the difference of a concave or convex (D.C.) structure, is used to deal with the non-convex programming.
(4) The performance of the proposed scheme is compared with the traditional orthogonal multiple access (OMA) scheme, which verifies the superiority of the proposed scheme in terms of energy efficiency.

The rest of the paper is organized as follows. The system model and the optimization problem are introduced in Section 2. Then, in Section 3, we provide the proposed optimal solution. The simulation analysis and relevant discussion are displayed in Section 4. Lastly, a brief summary of this paper is presented in Section 5.

2. System Model and Problem Formulation

In this section, we present the system model first and, subsequently, discuss the construction of the optimization problem.

2.1. System Model

In this subsection, the system model of FD D2D communications underlaying cellular networks with downlink NOMA is presented, as shown in Figure 1. A downlink resource allocation scene is considered where two NOMA users (C_1 and C_2) share the downlink spectrum with a pair of D2D users (D_1 and D_2) in a single cell system. The same spectrum is accommodated to C_1 and C_2, utilizing the power multiplexing of NOMA. Therefore, the BS and two NOMA users are both equipped with a single antenna. In particular, the D2D users operate in FD mode and we assume that both D2D users are equipped with separate transmit and receive antennas.

We denote the channels of the BS-C_1, BS-C_2, BS-D_1, BS-D_2, D_1-D_2, D_2-D_1, D_1-C_1, D_1-C_2, D_2-C_1 and D_2-C_2 links as g_{b,c_1}, g_{b,c_2}, g_{b,d_1}, g_{b,d_2}, g_{d_1,d_2}, g_{d_2,d_1}, g_{d_1,c_1}, g_{d_1,c_2}, g_{d_2,c_1} and g_{d_2,c_2}, respectively. In addition, we assume that large-scale fading based on the distance path loss model and small-scale fading based on the Rayleigh fading model is the channel model [24]. We further assume that a dedicated control channel is applied to collect the channel state information (CSI) in our networks so that the perfect CSI is assumed. We denote that the transmission power from the BS to C_1 and C_2 are P_{c_1} and P_{c_2}. Accordingly, the transmit powers of the D_1 and D_2 are denoted by P_{d_1} and P_{d_2}, respectively.

To ensure that the SIC process at the two NOMA downlink users are successful, the users are sorted based on their channel gains, such that $g_{b,c_1} > g_{b,c_2}$. According to this order, C_1 first carries out SIC technology to eliminate interference from other users and

then decodes its own signal, while C_2 decodes its own signal by directly treating other signals as interference. The received signals of C_1 and C_2 are accordingly represented as

$$y_{c_1} = \sqrt{P_{c_1} g_{b,c_1}} x_{c_1} + \sqrt{P_{c_2} g_{b,c_1}} x_{c_2} + \sqrt{P_{d_1} g_{d_1,c_1}} x_{d_1} + \sqrt{P_{d_2} g_{d_2,c_1}} x_{d_2} + n_{c_1} \quad (1)$$

$$y_{c_2} = \sqrt{P_{c_1} g_{b,c_2}} x_{c_1} + \sqrt{P_{c_2} g_{b,c_2}} x_{c_2} + \sqrt{P_{d_1} g_{d_1,c_2}} x_{d_1} + \sqrt{P_{d_2} g_{d_2,c_2}} x_{d_2} + n_{c_2} \quad (2)$$

where x_{c_1}, x_{c_2}, x_{d_1} and x_{d_2} are the transmission signals of users c_1, c_2, d_1 and d_2, respectively, and $n_{c_1}, n_{c_2} \sim \mathcal{CN}(0, \sigma^2)$ denote additive white Gaussian noise (AWGN) with zero mean and σ^2 variance.

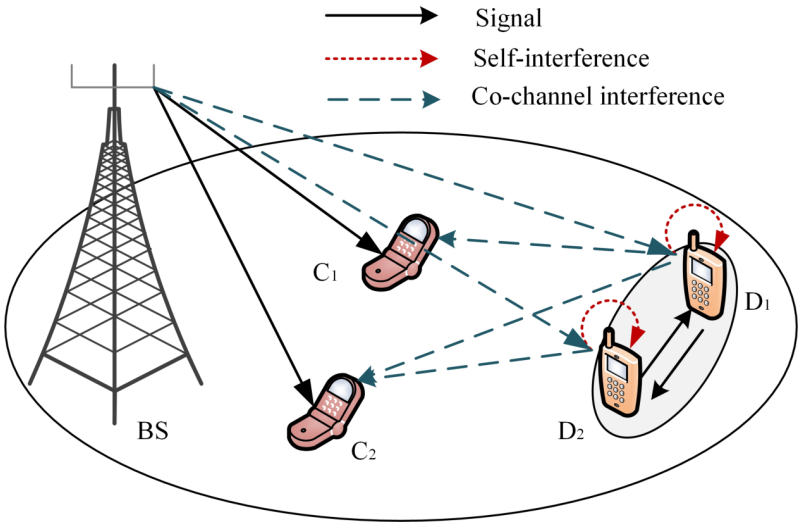


Figure 1. System model.

User c_1 first applies SIC technology to eliminate interference and then decodes its own signal, i.e.,

$$\tilde{\gamma}_{c_2} = \frac{P_{c_2} g_{b,c_1}}{P_{c_1} g_{b,c_1} + P_{d_1} g_{d_1,c_1} + P_{d_2} g_{d_2,c_1} + \sigma^2} \quad (3)$$

$$\gamma_{c_1} = \frac{P_{c_1} g_{b,c_1}}{P_{d_1} g_{d_1,c_1} + P_{d_2} g_{d_2,c_1} + \sigma^2} \quad (4)$$

where $\tilde{\gamma}_{c_2}$ and γ_{c_1} are the signal-to-interference and noise ratio (SINR) of user C_2 at user C_1 and user C_1, respectively.

To make the SIC process successful at the C_1, the transmission power of two NOMA users should meet the following requirement [25,26]:

$$\frac{(P_{c_2} - P_{c_1}) g_{b,c_1}}{P_{d_1} g_{d_1,c_1} + P_{d_2} g_{d_2,c_1} + \sigma^2} \geq \theta \quad (5)$$

where θ represents the minimum power gap, ensuring that the SIC process is successful between the two NOMA users.

As for user C_2, it decodes the received signal x_{c_2} directly while treating other received signals as interference. Therefore, the SINR γ_{c_2} of user C_2 is

$$\gamma_{c_2} = \frac{P_{c_2} g_{b,c_2}}{P_{c_1} g_{b,c_2} + P_{d_1} g_{d_1,c_2} + P_{d_2} g_{d_2,c_2} + \sigma^2} \quad (6)$$

Similarly, the received signals of D2D users are denoted as

$$y_{d_1} = \sqrt{P_{c_1} g_{b,d_1}} x_{c_1} + \sqrt{P_{c_2} g_{b,d_1}} x_{c_2} + \sqrt{P_{d_2} g_{d_2,d_1}} x_{d_2} + \sqrt{\eta P_{d_1}} x_{d_1} + n_{d_1} \tag{7}$$

$$y_{d_2} = \sqrt{P_{c_1} g_{b,d_2}} x_{c_1} + \sqrt{P_{c_2} g_{b,d_2}} x_{c_2} + \sqrt{P_{d_1} g_{d_1,d_2}} x_{d_1} + \sqrt{\eta P_{d_2}} x_{d_2} + n_{d_2} \tag{8}$$

where ηP_{d_1} and ηP_{d_2} are the residual SI of D_1 and D_2, and η denotes the SI cancellation capability of the FD transmitter. n_{d_1} and n_{d_2} denote AWGN with zero mean and σ^2 variance. Thus, the received SINRs γ_{d_1} and γ_{d_2} at users D_1 and D_2 are, respectively, represented as

$$\gamma_{d_1} = \frac{P_{d_2} g_{d_2,d_1}}{P_{c_1} g_{b,d_1} + P_{c_2} g_{b,d_1} + \eta P_{d_1} + \sigma^2} \tag{9}$$

$$\gamma_{d_2} = \frac{P_{d_1} g_{d_1,d_2}}{P_{c_1} g_{b,d_2} + P_{c_2} g_{b,d_2} + \eta P_{d_2} + \sigma^2} \tag{10}$$

2.2. Problem Formulation

The energy efficiency optimization problem is formulated mathematically in this subsection while ensuring users' QoS requirements, power constraints and the minimum gap for successful SIC.

Based on Equations (4), (5), (9) and (10), considering the unit bandwidth, the transmission rate corresponding to the user i can be expressed as

$$R_i = \log_2(1 + \gamma_i) \tag{11}$$

where $i \in \mathcal{U}, \mathcal{U} = \{c_1, c_2, d_1, d_2\}$.

The energy efficiency of the FD D2D communication underlaying cellular networks with downlink NOMA can be expressed as the ratio of the system sum rate to the total power consumption. The total power consumption consists of average circuit loss power P_0 and the transmit power of BS and D2D users. Therefore, the following linear model is applied to represent the power consumption

$$P_{sum} = \sum_{i \in \mathcal{U}} P_i + 3P_0 \tag{12}$$

where $3P_0$ is the circuit power at the BS and users D_1 and D_2.

Maximizing the system's energy efficiency is our purpose while satisfying three kinds of constraints. Firstly, we ensure the minimum transmission rate of each user as a QoS requirement. Secondly, the transmit power of all users is constrained. In addition to the above two common constraints, we also guarantee the successful SIC constraint for NOMA user C_1. The energy efficiency optimization problem can be expressed as follows:

$$\max_{P_i} \ \frac{\sum_{i \in \mathcal{U}} R_i}{\sum_{i \in \mathcal{U}} P_i + 3P_0} \tag{13a}$$

$$s.t. \quad R_{c_1} \geq R_{th1}, R_{c_2} \geq R_{th2} \tag{13b}$$

$$R_{d_1}, R_{d_2} \geq R_{thd} \tag{13c}$$

$$(P_{c_2} - P_{c_1})k \geq \theta \tag{13d}$$

$$P_{c_1} + P_{c_2} \leq P_{bmax} \tag{13e}$$

$$0 \leq P_{d_1}, P_{d_2} \leq P_{dmax} \tag{13f}$$

$$P_{c_1}, P_{c_2} \geq 0 \tag{13g}$$

where Equation (13a) is the objective function of the system's energy efficiency maximization. R_{th1} and R_{th2} in (13b) are the minimum transmission rates of C_1 and C_2, respectively.

Since the channel gain of C_2 is worse than that of C_1, we set $R_{th2} < R_{th1}$. R_{thd} in (13c) is the QoS requirements for D_1 and D_2. Additionally, the constraint in (13d) ensures that the SIC process of C_1 is successful and k is the normalized coefficient, $k = \frac{g_{b,c_1}}{P_{d_1} g_{d_1,c_1} + P_{d_2} g_{d_2,c_1} + \sigma^2}$. In the constraints found in (13e) and (13f), P_{bmax} and P_{dmax} are the maximum transmission powers of the BS and the D2D users, respectively.

3. Proposed Optimal Solution

In this section, the power allocation of the optimization problem (13a) for FD D2D communications underlaying cellular networks with downlink NOMA is researched. Note that the optimization problem (13a) is a non-convex and non-linear fractional problem, which makes it quite difficult to obtain the optimal solution directly. Consequently, a dual-layer iteration algorithm is proposed to deal with the problem. The outer-layer iteration algorithm is to solve the non-linear fractional objective function based on Dinkelbach algorithm. After that, the objective function is still a non-convex optimization because the substructure has the D.C. structure. Therefore, the inner-layer iteration algorithm is to solve the non-convex optimization problem based on the D.C. programming. Thus, the non-convex and non-linear fractional objective function is transformed into a convex function and we can apply convex optimization to gain the optimal power allocation solution. There is no further improvement in the system's energy efficiency when the iterative process is convergent.

3.1. Outer-Layer Iteration Algorithm

For the purpose of solving the objective optimization problem, which is a non-convex and non-linear fractional programming, we mainly focus on transforming the form of the objective function in this subsection, and we assume that the optimal solution of Equation (13a) is λ^*, which is given by

$$\lambda^* = \max_{P_i^*} \frac{\sum_{i \in \mathcal{U}} R_i}{\sum_{i \in \mathcal{U}} P_i + 3P_0} \tag{14}$$

where P_i^* is the optimal power allocation. The following proven Theorem 1 can help us transform the objective function [31,32].

Theorem 1. *Suppose* $F(\lambda) = \max_{P_i} \sum_{i \in \mathcal{U}} R_i - \lambda(\sum_{i \in \mathcal{U}} P_i + 3P_0)$, *then,* $F(\lambda)$ *is a monotonically decreasing function of* λ, *and the maximum energy efficiency* $\lambda^* = \max_{P_i^*} \frac{\sum_{i \in \mathcal{U}} R_i}{\sum_{i \in \mathcal{U}} P_i + 3P_0}$ *is obtained if and only if*

$$\max_{P_i} \sum_{i \in \mathcal{U}} R_i - \lambda^* (\sum_{i \in \mathcal{U}} P_i + 3P_0) = 0 \tag{15}$$

Hence, based on Theorem 1, we can transform the non-linear fractional programming of Equation (13a) to the problem of Equation (16). Thus, we can solve Equation (16) to obtain the corresponding optimal power allocation:

$$\max_{P_i} \sum_{i \in \mathcal{U}} R_i - \lambda (\sum_{i \in \mathcal{U}} P_i + 3P_0) \quad s.t.\ \mathcal{D} \tag{16}$$

where $\mathcal{D}$ is the set consisting of Equations (13b)–(13g). As for constraints (13b)–(13d), we can transform them into a linear form of power, respectively, in Equation (17). Therefore, the set $\mathcal{D}$ is a convex set:

$$\begin{cases} P_{c_1}g_{b,c_1} - (2^{R_{th1}} - 1)(P_{d_1}g_{d_1,c_1} + P_{d_2}g_{d_2,c_1} + \sigma^2) \geq 0 \\ P_{c_2}g_{b,c_2} - (2^{R_{th2}} - 1)(P_{c_1}g_{b,c_2} + P_{d_1}g_{d_1,c_2} + P_{d_2}g_{d_2,c_2} + \sigma^2) \geq 0 \\ P_{d_1}g_{d_1,d_2} - (2^{R_{thd}} - 1)(P_{c_1}g_{b,d_2} + P_{c_2}g_{b,d_2} + \eta P_{d_2} + \sigma^2) \geq 0 \\ P_{d_2}g_{d_2,d_1} - (2^{R_{thd}} - 1)(P_{c_1}g_{b,d_1} + P_{c_2}g_{b,d_1} + \eta P_{d_1} + \sigma^2) \geq 0 \\ g_{b,c_1}(P_{c_2} - P_{c_1}) - \theta(P_{d_1}g_{d_1,c_1} + P_{d_2}g_{d_2,c_1} + \sigma^2) \geq 0 \end{cases} \tag{17}$$

Based on the above analysis, we have solved the non-linear fractional objective optimization problem. But we cannot obtain the optimal solution by applying the outer-layer iteration algorithm because the substructure $\sum_{i\in\mathcal{U}} R_i$ is still a non-convex structure. Therefore, in next subsection, we will introduce the transform of the non-convex structure and then present the complete iteration algorithm, including outer-layer iteration and inner-layer iteration.

3.2. Inner-Layer Iteration Algorithm

Although we have transformed the non-linear fractional function in Equation (13a), the subtraction structure $\sum_{i\in\mathcal{U}} R_i$ in problem Equation (16) is still a non-convex structure that needs to be transformed into a convex structure.

First, we rewrite the subtraction structure $\sum_{i\in\mathcal{U}} R_i$ as

$$\sum_{i\in\mathcal{U}} R_i = f_1(\mathbf{P}) - f_2(\mathbf{P}) \tag{18}$$

where,

$$\begin{cases} f_1(\mathbf{P}) = \log_2(A_1) + \log_2(B_1) + \log_2(C_1) + \log_2(D_1) \\ A_1 = P_{c_1}g_{b,c_1} + P_{d_1}g_{d_1,c_1} + P_{d_2}g_{d_2,c_1} + \sigma^2 \\ B_1 = P_{c_2}g_{b,c_2} + P_{c_1}g_{b,c_2} + P_{d_1}g_{d_1,c_2} + P_{d_2}g_{d_2,c_2} + \sigma^2 \\ C_1 = P_{d_1}g_{d_1,d_2} + P_{c_1}g_{b,d_2} + P_{c_2}g_{b,d_2} + \eta P_{d_2} + \sigma^2 \\ D_1 = P_{d_2}g_{d_2,d_1} + P_{c_1}g_{b,d_1} + P_{c_2}g_{b,d_1} + \eta P_{d_1} + \sigma^2 \end{cases} \tag{19}$$

and

$$\begin{cases} f_2(\mathbf{P}) = \log_2(A_2) + \log_2(B_2) + \log_2(C_2) + \log_2(D_2) \\ A_2 = P_{d_1}g_{d_1,c_1} + P_{d_2}g_{d_2,c_1} + \sigma^2 \\ B_2 = P_{c_1}g_{b,c_2} + P_{d_1}g_{d_1,c_2} + P_{d_2}g_{d_2,c_2} + \sigma^2 \\ C_2 = P_{c_1}g_{b,d_2} + P_{c_2}g_{b,d_2} + \eta P_{d_2} + \sigma^2 \\ D_2 = P_{c_1}g_{b,d_1} + P_{c_2}g_{b,d_1} + \eta P_{d_1} + \sigma^2 \end{cases} \tag{20}$$

Obviously, $f_1(\mathbf{P})$ and $f_2(\mathbf{P})$ are both concave functions on $\mathbf{P}$, and the second part $\lambda(\sum_{i\in\mathcal{U}} P_i + 3P_0)$ in Equation (16) is a linear function. Therefore, the objective function in (16) has the D.C. structure. In addition, $\mathcal{D}$ is a convex set. Thus, we can solve the problem (16) based on D.C. programming.

According to [26], $f_2(\mathbf{P})$ can be expanded by the first-order Taylor function around $\mathbf{P}^{(k)}$:

$$f_2(\mathbf{P}) = f_2(\mathbf{P}^{(k)}) + \langle \bigtriangledown f_2(\mathbf{P}^{(k)}), \mathbf{P} - \mathbf{P}^{(k)} \rangle \tag{21}$$

where $\langle \mathbf{x}, \mathbf{y} \rangle = \mathbf{x}^T\mathbf{y}$ is the inner product of the vectors $\mathbf{x}$ and $\mathbf{y}$. $\bigtriangledown f_2(\mathbf{P}^{(k)})$ is the gradient of $f_2(\mathbf{P})$ at $\mathbf{P}^{(k)}$.

Therefore, the objective function in problem Equation (16) can be transformed to a concave function, which is expressed as:

$$\max_{\mathbf{P}} \; f_1(\mathbf{P}) - f_2(\mathbf{P}^{(k)}) - \langle \bigtriangledown f_2(\mathbf{P}^{(k)}), \mathbf{P} - \mathbf{P}^{(k)} \rangle - \lambda P_{sum} \quad s.t. \; \mathcal{D} \tag{22}$$

It is easy to solve the concave problem in Equation (22) by applying standard convex optimization techniques, such as the interior-point method [33].

The detailed dual-layer iteration algorithm to solve the optimization problem (22) is shown in Algorithm 1. First, we set the initial conditions of the optimization problem (22). Then, the outer-layer iteration updates λ constantly and the inner-layer iteration updates the power $\mathbf{P}^*$ until the inner-layer iteration and outer-layer iteration meet the tolerances, respectively. Finally, the optimal solution can be obtained through Algorithm 1 after a finite number of iterations [31].

Algorithm 1 Complete Dual-layer Iteration Algorithm

Outer-layer iteration algorithm

Initialization: Set $m = 0$, tolerance $\zeta_1 > 0$ and $\mathbf{P}^{(0)} \in \mathcal{D}$ is a feasible solution of optimization problem (22), then obtain $\lambda^{(0)} = \max\limits_{\mathbf{P}^{(0)}} \frac{\sum_{i \in \mathcal{U}} R_i}{\sum_{i \in \mathcal{U}} P_i + 3P_0}$

Repeat

1: perform **Inner-layer iteration algorithm** with $\lambda^{(m)}$ and obtain the optimal solution $\lambda^{(m+1)}$
2: Set $m = m + 1$
3: **Until** $|F(\lambda^{(m)})| < \zeta_1$
4: **Return** $\lambda^{(m)}$

Inner-layer iteration algorithm

Initialization: Set $n = 0$, tolerance $\zeta_2 > 0$ and $\mathbf{P}^{(0)} \in \mathcal{D}$ is a feasible solution of optimization problem (22)

Repeat

5: Solve optimization problem (22) with $\mathbf{P}^{(n)}$ and obtain the optimal solution $\mathbf{P}^{(n+1)}$
6: Set $n = n + 1$
7: **Until** $|\mathbf{P}^{(n)} - \mathbf{P}^{(n-1)}| < \zeta_2$
8: **Return** $\mathbf{P}^{(n)}$

4. Simulation Results

We provide the simulation analysis in this section, which illustrates the superiority of the system's energy efficiency for the proposed scheme. Firstly, we analyze the convergence of the iterative algorithm in Section 3. Next, we further analyze the impact of the QoS requirement of each user, the minimum gap for successful SIC and SI cancellation coefficient on the system's energy efficiency. For comparison, we present the simulation results with traditional OMA networks where each cellular user occupies half-spectrum resources and D2D users share the total spectra at the same time. Furthermore, the achievable rate of each user is still an important metric to the system performance. Therefore, we analyze the effect of SI cancellation coefficient and the distance between D2D users on the user's achievable rate, and compare FD D2D with HD D2D to observe the improvement of the achievable sum rate.

The channel model between user i and user j is denoted as $g_{i,j} = d_{i,j}^{-\alpha}|h_{i,j}|^2$. Among them, $d_{i,j}^{-\alpha}$ is the distance path loss, in which $d_{i,j}$ represents the distance from the transmitter i to the receiver j in meters, α represents the path loss coefficient and we set $\alpha = 4$. For the small-scale fading, all users experience independent Rayleigh fading with zero mean and unit variance. Particularly, all terminals are uniformly distributed in the cell with a radius of 400 m and the D2D users are located within a short distance of 40 m. Furthermore, we set $R_{th1} = 3$ bps, $R_{th2} = 1$ bps, $R_{thd} = 3$ bps, $P_{bmax} = 24$ dBm and $P_{dmax} = 21$ dBm. Unless stated otherwise, Table 1 presents the simulation parameters applied in this paper.

Table 1. Simulation parameters.

Parameter	Value
Cell radius	400 m
Channel bandwidth	1 Hz
Path loss exponent, α	4
Minimum power gap for successful SIC, θ	10 dBm
Minimum rate requirement of C_1, R_{th1}	3, 5 bps
Minimum rate requirement of C_2, R_{th2}	1, 1.5 , . . . , 3 bps
Minimum rate requirement of D2D, R_{thd}	3, 5 bps
Circuit power, P_0	17 dBm
Tolerance, ζ_1, ζ_2	10^{-4}
Noise density, σ^2	-169 dBm
Maximum power of BS, P_{bmax}	24 dBm
Maximum power of D2D, P_{dmax}	21 dBm
SI cancellation coefficient, η	$-110, -105, \ldots, -70$ dB
Maximum distance between D2D users	40 m

The convergence performance of the proposed dual-layer iteration algorithm to obtain the optimal power allocation was researched and is presented in Figure 2. It can be observed that the system's energy efficiency converges to a stable value after finite iterations (four times), which indicates that the iterative algorithm we proposed in Section 3 has a lightweight and less complex nature. In addition, the reduction in the maximum transmission power of BS and D2D users will lead to the reduction in system's energy efficiency. This is because the reduction in the maximum transmission power will lead to the reduction in the power that can be allocated during the transmission, which will reduce the reachable rate of the users, thus reducing the system's energy efficiency. We can also see that the reduction in the maximum transmission power of the BS has a greater influence on the energy efficiency than that of D2D users. This is because when the transmission power of the BS decreases, the BS still needs to allocate more power to maintain the minimum rate of the NOMA weak user C_2, while allocating less power to NOMA strong user C_1, hence reducing the system's energy efficiency.

Then, the system's energy efficiency is investigated with variable circuit power and minimum gap for successful SIC in Figure 3. We can determine that when the circuit power increases, the system's energy efficiency decreases, and the proposed scheme always outperforms the OMA scheme, which proves the advantage of our proposed scheme and the feasibility of the solution. In addition, when θ increases, the system's energy efficiency of the proposed scheme shows a downward trend. This is because more power should be allocated to the poor channel gain user C_2 and accordingly less power to the strong channel gain user C_1, which will lessen the system's energy efficiency. Moreover, because the energy efficiency of the OMA scheme is independent of the minimum gap for a successful SIC, we only show one curve of the OMA communication scheme.

The effect of the QoS requirements of users on the system's energy efficiency is depicted in Figure 4, where $\eta = -90$ dB. We can see the proposed scheme also outperforms the OMA scheme. In addition, when the minimum transmission rate of user C_2 increases, the energy efficiency of all cases presents a downward trend. This is because when the minimum transmission rate of C_2 increases, the BS will allocate more power to C_2 to maintain the minimum requirement. Then, the power allocated to C_1 will inevitably decrease, which will reduce the system sum rate and then reduce the system's energy efficiency. Accordingly, when the minimum transmission rate of user C_1 increases, the system's energy efficiency also decreases. This is because the increase in the minimum transmission rate of C_1 will cause the BS to allocate more power to user C_1, which will lead to the insufficient power allocated to user C_2 to maintain the normal communication, thus reducing the energy efficiency of the system.

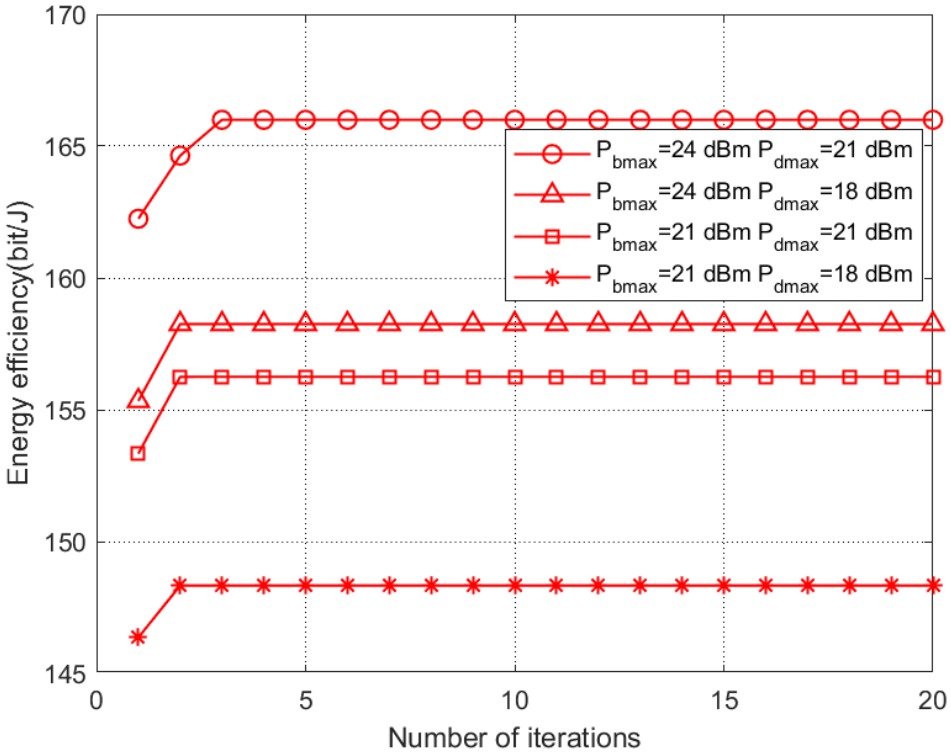


Figure 2. The energy efficiency of the system versus number of iterations.

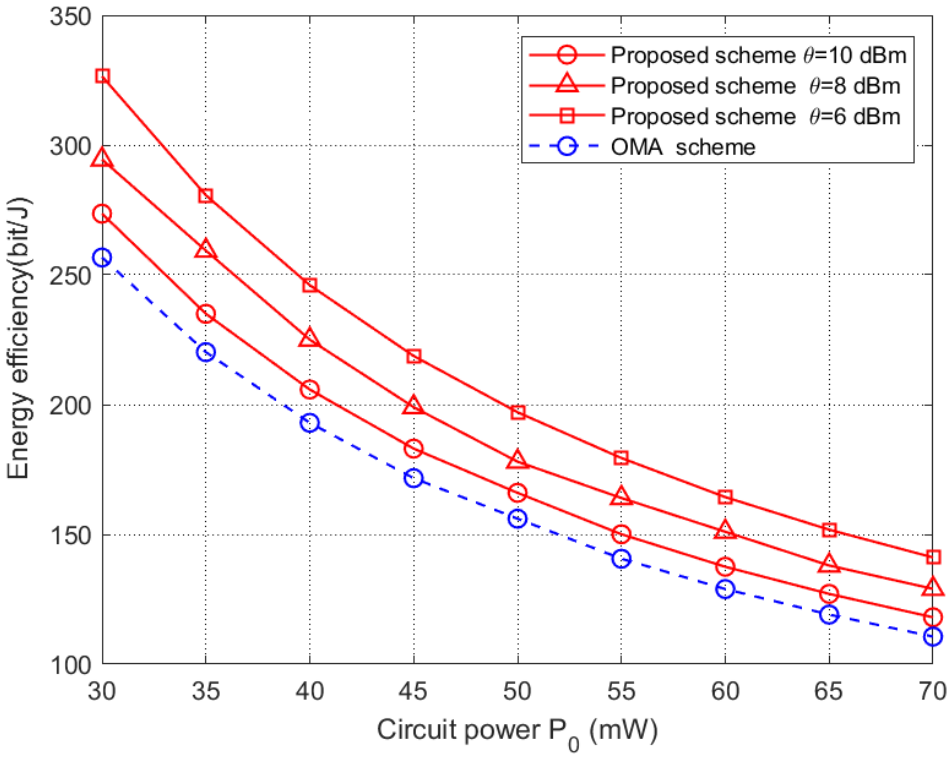


Figure 3. The energy efficiency of the system versus circuit power.

We present the effects of different minimum transmission rates of D2D users and the SI cancellation coefficient on the system's energy efficiency in Figure 5. We observe that as SI decreases, the energy efficiency of all cases increases. Furthermore, with the increase in R_{thd}, the energy efficiency of the system decreases, no matter in the proposed scheme or the OMA scheme. This is because with the increase in the minimum transmission rate

of D2D users, the transmission power of the D2D users also needs to increase. Therefore, the transmission power may not meet the requirements of the minimum transmission rate, resulting in the reduction in the system's energy efficiency.

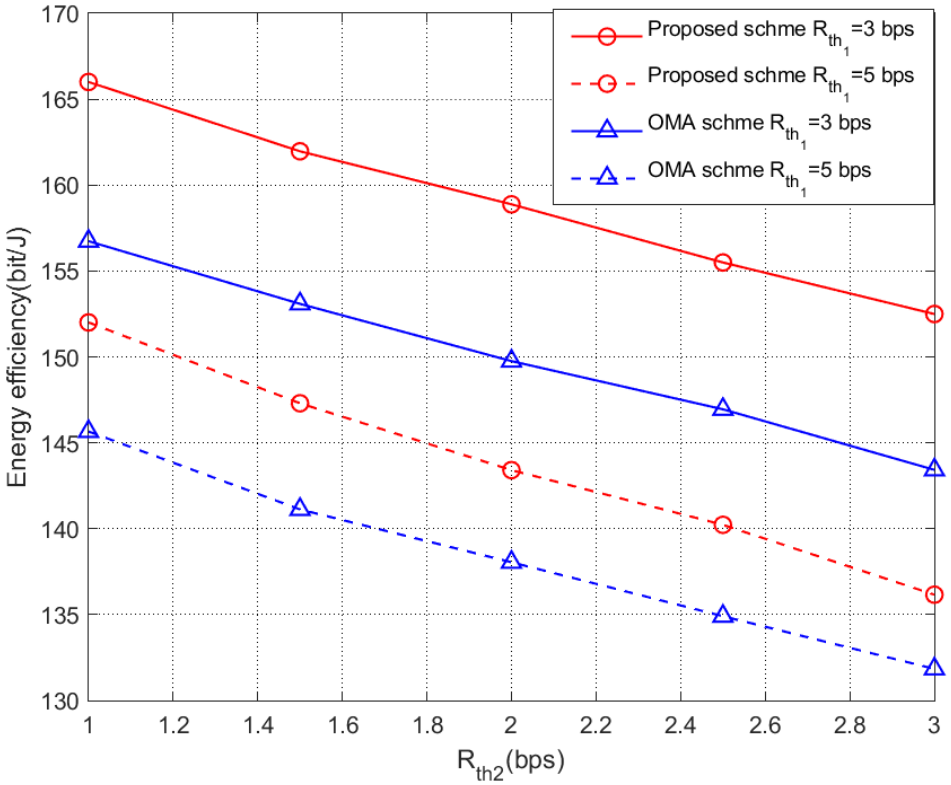


Figure 4. The energy efficiency of the system versus the minimum transmission rate of C_2.

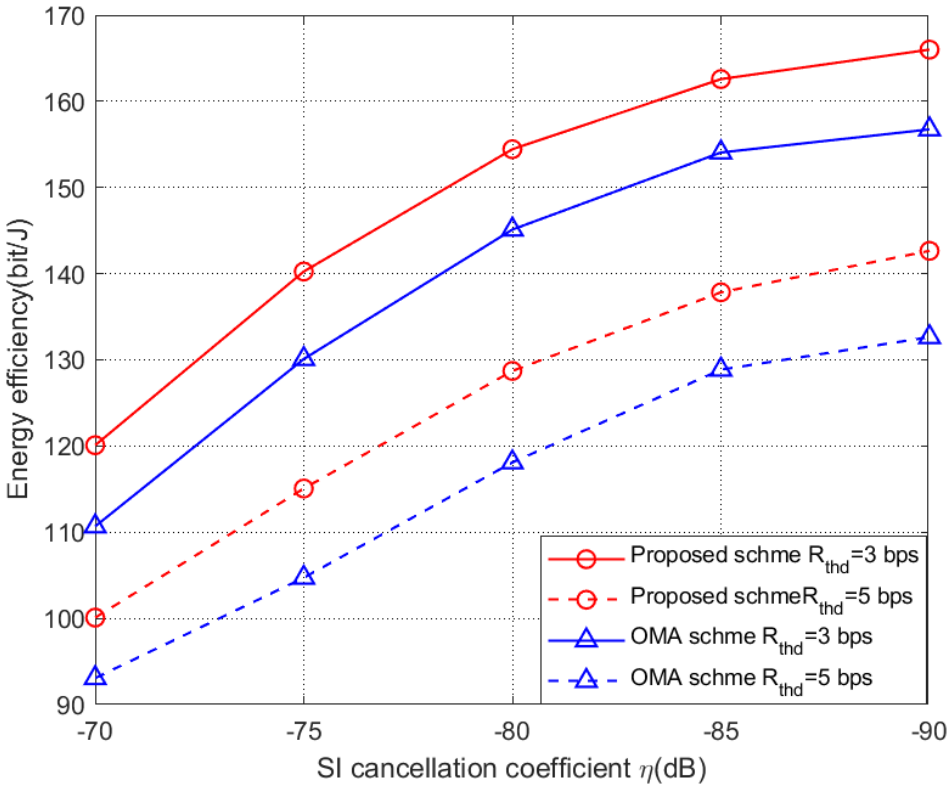


Figure 5. The energy efficiency of the system versus the SI cancellation coefficient.

Although we aim to maximize the system's energy efficiency in this paper, the spectral efficiency of the users is still a key metric that affects communication quality between users. In Figure 6, we have illustrated the relationship between the user's achievable rate and the SI cancellation coefficient. We can see that when η varies, the achievable rate of each user meets the minimum transmission rate requirement. Particularly, C_2 always maintains the minimum threshold, while C_1's rate decreases and D2D users' rate increases. This is because SI only exists in FD D2D users. Obviously, when η decreases, the achievable rate of D2D users increases. In the meantime, in order to optimize the overall energy efficiency, the D2D users must allocate more power, which means more co-channel interference to the cellular users. Hence, C_1's rate gradually decreases and C_2's rate consistently keeps to the minimum in order to maintain QoS requirement.

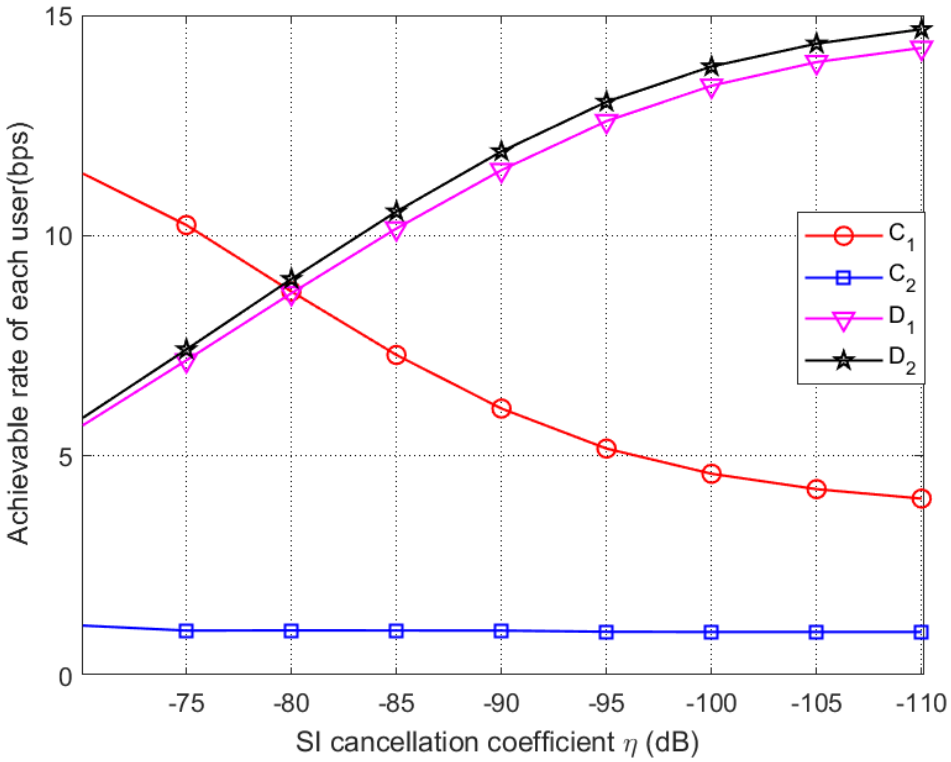


Figure 6. The achievable rate of each user versus the SI cancellation coefficient.

Figure 7 discusses the effect of the distance between D2D users on the ergodic sum rate. In addition to comparing with the OMA scheme in Figure 7, we also change the FD D2D users to HD D2D users for comparison in order to discuss the influence of SI cancellation coefficient on the system sum rate, herein, namely the HD-D2D scheme. We can see the system sum rate of all cases decrease as the D2D distance increases, because the channel condition of the users becomes worse, reducing the system sum rate. From the figure, we also find out that our proposed scheme has advantages over the other two schemes with regard to the sum rate.

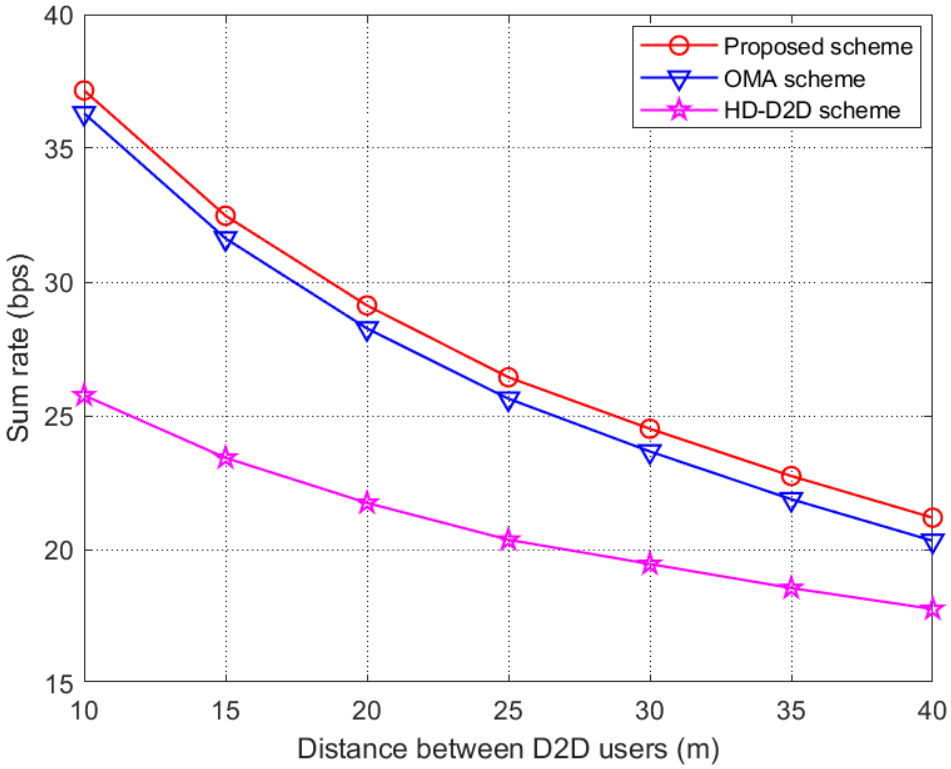


Figure 7. The sum rate of the system versus the distance between D2D users.

5. Conclusions

In this paper, we proposed a dual-layer iteration power allocation algorithm to maximize the energy efficiency of the system, where one FD D2D user pair uses the same spectrum resource with two cellular users using a power domain NOMA transmission. The outer-layer iteration is to solve a non-linear fractional problem for energy efficiency based on Dinkelbach and the inner-layer iteration is to solve the non-convex optimization for power allocation based on the D.C. programming. The simulation results show that the proposed algorithm can achieve better energy efficiency than the traditional OMA with the constraints of the successful SIC power level for NOMA users, the QoS requirements and maximal transmission power of D2D users and BS. Although an improved performance is achieved, there are still some challenges to be solved for more complex interference scenarios. In the near future, we will focus on extending our proposed algorithm to the scenario of multiple NOMA groups sharing a spectrum with multiple D2D user pairs by jointly considering channel assignment and power allocation to maximize the system's energy efficiency. Moreover, machine learning methods can be further introduced to solve the joint optimization problem.

Author Contributions: Conceptualization, X.Z., F.L., Y.Z., S.C. and J.G.; Investigation, S.C.; Methodology, F.L.; Software, Y.Z.; Writing—original draft, F.L. and Y.Z.; Writing—review and editing, X.Z. All authors have read and agreed to the published version of the manuscript.

Funding: This work was supported by the High Quality Development of the Manufacturing Industry Special Project, grant number TC220H07A.

Institutional Review Board Statement: Not applicable.

Informed Consent Statement: Not applicable.

Data Availability Statement: Not applicable.

Conflicts of Interest: The authors have no relevant financial or non-financial interest to disclose.

References

1. Li, L.; Hu, Y.; Zhang, H.; Liang, W.; Gao, A. Deep learning based physical layer security of D2D underlay cellular network. *China Commun.* **2020**, *17*, 93–106.
2. Cai, Y.; Ni, Y.; Zhang, J.; Zhao, S.; Zhu, H. Energy efficiency and spectrum efficiency in underlay device-to-device communications enabled cellular networks. *China Commun.* **2019**, *16*, 16–34.
3. Gu, W.; Zhu, Q. Stackelberg Game Based Social-Aware Resource Allocation for NOMA Enhanced D2D Communications. *Electronics* **2019**, *8*, 1360. [CrossRef]
4. Sun, Y.; Wang, F.; Liu, Z. Coalition Formation Game for Resource Allocation in D2D Uplink Underlaying Cellular Networks. *IEEE Commun. Lett.* **2019**, *23*, 888–891. [CrossRef]
5. Yadav, A.; Quan, C.; Varshney, P.K.; Poor, H.V. On Performance Comparison of Multi-Antenna HD-NOMA, SCMA, and PD-NOMA Schemes. *IEEE Wireless Commun. Lett.* **2021** , *10*, 715–719. [CrossRef]
6. Huang, R.; Wan, D.; Ji, F.; Qing, H.; Li, J.; Yu, H.; Chen, F. Performance analysis of NOMA-based cooperative networks with relay selection. *China Commun.* **2020**, *17*, 111–119.
7. Liu, G.; Wang, Z.; Hu, J.; Ding, Z.; Fan, P. Cooperative NOMA Broadcasting/Multicasting for Low-Latency and High-Reliability 5G Cellular V2X Communications. *IEEE Internet Things J.* **2019**, *6*, 7828–7838. [CrossRef]
8. Mikhaylov, K.; Petrov, V.; Gupta, R.; Lema, M.A.; Galinina, O.; Andreev, S.; Koucheryavy, Y.; Valkama, M.; Pouttu, A.; Dohler, M. Energy Efficiency of Multi-Radio Massive Machine-Type Communication (MR-MMTC): Applications, Challenges, and Solutions. *IEEE Commun. Mag.* **2019**, *57*, 100–106.
9. Sabuj, S.R.; Ahmed, A.; Cho, Y.; Lee, K.-J.; Jo, H.-S. Cognitive UAV-Aided URLLC and mMTC Services: Analyzing Energy Efficiency and Latency. *IEEE Access* **2021**, *9*, 5011–5027. [CrossRef]
10. Lee, W.; Ban, T.-W.; Jung, B.C. Distributed Transmit Power Optimization for Device-to-Device Communications Underlying Cellular Networks. *IEEE Access* **2019**, *7*, 87617–87633.
11. Du, Y.; Zhang, W.; Wang, S.; Xia, J.; Mohammad, H.A. Joint Resource Allocation and Mode Selection for Device-to-Device Communication Underlying Cellular Networks. *IEEE Access* **2021**, *9*, 29020–29031. [CrossRef]
12. Wang, D.; Zhang, S.; Cheng, Q.; Zhang, X. Joint Interference Alignment and Power Allocation Based on Stackelberg Game in Device-to-Device Communications Underlying Cellular Networks. *IEEE Access* **2021**, *9*, 81651–81659. [CrossRef]
13. Awan, A.Y.; Ali, M.; Naeem, M.; Qamar, F.; Sial, M.N. Joint Network Admission Control, Mode Assignment, and Power Allocation in Energy Harvesting Aided D2D Communication. *IEEE Trans. Ind. Inform.* **2020**, *16*, 1914–1923. [CrossRef]
14. Zhang, R.; Jia, S.; Ma, Y.; Xu, C. Social-Aware D2D Video Delivery Method Based on Mobility Similarity Measurement in 5G Ultra-Dense Network. *IEEE Access* **2020**, *8*, 52413–52427. [CrossRef]
15. Al-kahtani, M.S.; Ferdouse, L.; Karim, L. Energy Efficient Power Domain Non-Orthogonal Multiple Access Based Cellular Device-to-Device Communication for 5G Networks. *Electronics* **2020**, *9*, 237. [CrossRef]
16. Alemaishat, S.; Saraereh, O.A.; Khan, I.; Choi, B.J. An Efficient Resource Allocation Algorithm for D2D Communications Based on NOMA. *IEEE Access* **2019**, *7*, 120238–120247. [CrossRef]
17. Budhiraja, I.; Kumar, N.; Tyagi, S.; Tanwar, S.; Han, Z. An Energy Efficient Scheme for WPCN-NOMA Based Device-to-Device Communication. *IEEE Trans. Veh. Technol.* **2021**, *70*, 11935–11948. [CrossRef]
18. Cheng, Y.; Liang, C.; Chen, Q.; Yu, F.R. Energy-Efficient D2D-Assisted Computation Offloading in NOMA-Enabled Cognitive Networks. *IEEE Trans. Veh. Technol.* **2021**, *70*, 13441–13446. [CrossRef]
19. Chen, J.; Jia, J.; Liu, Y.; Wang, X.; Aghvami, A.H. Optimal Resource Block Assignment and Power Allocation for D2D-Enabled NOMA Communication. *IEEE Access* **2019**, *7*, 90023–90035. [CrossRef]
20. Li, R.; Hong, P.; Xue, K.; Zhang, M.; Yang, T. Resource Allocation for Uplink NOMA-Based D2D Communication in Energy Harvesting Scenario: A Two-Stage Game Approach. *IEEE Trans. Wirel. Commun.* **2022**, *21*, 976–990. [CrossRef]
21. Do, D.-T.; Nguyen, M.-S.V.; Le, A.-T.; Rabie, K.M.; Zhang, J. Joint Full-Duplex and Roadside Unit Selection for NOMA-Enabled V2X Communications: Ergodic Rate Performance. *IEEE Access* **2020**, *8*, 140348–140360. [CrossRef]
22. Dang, H.-P.; Nguyen, M.-S.V.; Do, D.-T.; Pham, H.-L.; Selim, B.; Kaddoum, G. Joint Relay Selection, Full-Duplex and Device-to-Device Transmission in Wireless Powered NOMA Networks. *IEEE Access* **2020**, *8*, 82442–82460. [CrossRef]
23. Dinh, P.; Arfaoui, M.A.; Sharafeddine, S.; Assi, C.; Ghrayeb, A. Joint User Pairing and Power Control for C-NOMA with Full-Duplex Device-to-Device Relaying. In Proceedings of the 2019 IEEE Global Communications Conference (GLOBECOM), Waikoloa, HI, USA, 9–13 December 2019; pp. 1–6.
24. Duan, W.; Ji, Y.; Hou, J.; Zhuo, B.; Wen, M.; Zhang, G. Partial-DF Full-Duplex D2D-NOMA Systems for IoT with/without an Eavesdropper. *IEEE Internet Things J.* **2021**, *8*, 6154–6166. [CrossRef]
25. Li, J.; Li, X.; Wang, A.; Ye, N. Beamspace MIMO-NOMA for Millimeter-Wave Broadcasting via Full-Duplex D2D Communications. *IEEE Trans. Broadcast.* **2020**, *66*, 545–554. [CrossRef]
26. Chen, Y.; Zhang, G.; Xu, H.; Ren, Y.; Chen, X.; Li, R. Outage Constrained Design in NOMA-Based D2D Offloading Systems. *Electronics* **2022**, *11*, 256. [CrossRef]
27. Jiang, J.; Guo, J.; Khan, M. Energy-saving Service Offloading for the Internet of Medical Things Using Deep Reinforcement Learning. *ACM TOSN* **2023**, *19*, 1–20. [CrossRef]
28. Huang, H.; Yang, Y.; Ding, Z. Deep learning-based sum data rate and energy efficiency optimization for MIMO-NOMA systems. *IEEE Trans. Wirel. Commun.* **2020**, *8*, 5373–5388. [CrossRef]

29. Jiang, F.; Zhang, L.; Sun, C. Clustering and resource allocation strategy for D2D multicast networks with machine learning approaches. *China Commun.* **2021**, *18*, 196–211. [CrossRef]
30. Garcia, C.E.; Camana, M.R.; Koo, I. Ensemble Learning aided QPSO–Based Framework for Secrecy Energy Efficiency in FD CR-NOMA Systems. *IEEE Trans. Green Commun. Netw.* **2022**, *7*, 649–667. [CrossRef]
31. Dinkelbach, W. On nonlinear fractional programming. *Manag. Sci.* **1967**, *13*, 492–498. [CrossRef]
32. Ding, J.; Jiang, L.; He, C. Energy-Efficient Power Control for Underlaying Full-Duplex Device-to-Device Communications. In Proceedings of the 2017 Asia Modelling Symposium (AMS), Kota Kinabalu, Malaysia, 4–6 December 2017; pp. 155–160.
33. Xu, C.; Song, L.; Han, Z.; Zhao, Q.; Wang, X.; Cheng, X.; Jiao, B. Efficiency Resource Allocation for Device-to-Device Underlay Communication Systems: A Reverse Iterative Combinatorial Auction Based Approach. *IEEE J. Sel. Areas Commun.* **2013**, *31*, 348–358. [CrossRef]

Disclaimer/Publisher's Note: The statements, opinions and data contained in all publications are solely those of the individual author(s) and contributor(s) and not of MDPI and/or the editor(s). MDPI and/or the editor(s) disclaim responsibility for any injury to people or property resulting from any ideas, methods, instructions or products referred to in the content.